Effect of Phenyl-Capping and Dimer Formation on the Electronic States of CdS Nanoparticles by Means of Semiempirical Molecular Orbital Calculations

Yoshio Nosaka* and Hiroshi Tanaka

Department of Chemistry, Nagaoka University of Technology, Nagaoka, 940-2188, Japan

Received: September 10, 2001; In Final Form: January 2, 2002

A semiempirical molecular orbital calculation (MOPAC-PM3) was applied to investigate the effects of crystal arrangement, phenyl capping, and dimer formation for CdS nanoparticles. Molecular structures of possible polynuclear cadmium complexes were classified into four categories, zinc blende (ZB) tetrahedron, ZB cuboctahedron, wurtzite (W), and ZB−W mixture, and the last one is found to be the most favorable formation. The first excitation energies for these cluster complexes were calculated as the HOMO−LUMO energy difference and compared with the absorption peak energy reported in the literature. The electronic effect in polynuclear Cd thiophenolate complexes was discussed in terms of the fractionated density of states as an anti-π-bond interaction between the benzene π-orbital and the S 3p-orbitals. The dimer formation did not affect significantly the excited state of the nanoparticle dimer based on the estimation of intramolecular electron interaction.

Semiconductor nanoparticles have attracted much interest of researchers in basic science and applied materials.[1] Change in the electronic properties with size confinement is the origin of the unique properties of semiconductor nanoparticles. Investigation of the electronic structure of nanoparticles is possible by means of quantum chemical methods, explicitly using the molecular presentation. Since the chemical structure of polynuclear metal complex is clearly presented, it is a suitable model to investigate the electronic states of semiconductor nanoparticles. Some molecular orbital (MO) approaches to understand the electronic state of inorganic semiconductor nanoparticles have been reported so far, by using extend Hueckel,[2] CNDO/2,[3] CNDO/S,[4] and ab initio[5] methods for CdS nanocrystals. The extend Hueckel approach to Cd_xS_y clusters of zinc blende structure, where $x \leq 20$ and $y \leq 35$, has showed the decrease in HOMO−LUMO energy difference.[2] The CNDO/2 method is used to investigate surface defects of CdS nanocrystal with 221 Cd atoms.[3] Calculation of the oscillator strength of CdS nanoparticles has been tried by means of the CNDO/S method.[4] Ab initio calculation for a CdS cluster of tetrahedral symmetry up to Cd_{13} sulfide clusters allowed us to compare the bond length to the experimental values.[5] All reported MO calculations were performed for clusters with terminating hydrogen or without other atoms. However, real nano lusters are often capped with organic molecules, which may induce some effect on the electronic states of nanoparticles. For CdSe clusters containing ligand molecules, a density functional theory (DFT) approach to the synthesized clusters displayed the effect encountered in the transition from molecules to the solid state.[6] Since we are much interested in the interaction of inorganic CdS surface and capped organic molecules,[7] we applied a semiempirical MO method, PM3 in the MOPAC series, to investigate the electronic interaction between organic molecules and CdS particles. In this report, at first we applied this calculation method to describe the structure and energy levels of the thiolate complexes containing up to 35 Cd atoms, next the effect of capping with thiophenol was shown as an electronic interaction, and finally the cluster−cluster interaction in a nanoparticle dimer was discussed.

* Corresponding author. Tel/Fax: +81-258-47-9315. E-mail: nosaka@nagaokaut.ac.jp.

Polynuclear Cadmium Complexes and CdS Clusters. We constructed a series of model molecules of polynuclear Cd complexes to calculate the electronic states of nanoparticles. Two arrangements, zinc blende (ZB) and wurtzite (W), are known in CdS crystal. ZB and W arrangements can be recognized by the three consecutive bonds lying on a plane making a Z-shape (zigzag) and E-shape (crank), respectively. Although naturally abundant CdS crystal is of wurtzite structure, multinuclear Cd thiolate complex appeared in the literature showing ZB arrangement in their chemical bonds. Almost all nanoparticles reported also have the ZB structure.[8] To know the difference, CdS nanoclusters are classified into four groups on the basis of the bond conformation of the crystallographical arrangement. That is, (1) ZB tetrahedron or triangular pyramid, (2) ZB cuboctahedron, (3) wurtzite cluster, and (4) ZB−W mixed structure. Description for each series of the classified clusters is as follows.

(1) ZB Tetrahedron. The minimum size in the clusters of ZB tetrahedron structure is $[Cd_4(SR)_{10}]^{2-}$, where four Cd atoms locate at the vertex of the triangular pyramid.[9] This cluster has the same framework as adamantane ($C_{10}H_{16}$). When one Cd atom is placed between the two of the four Cd atoms, a decanuclear Cd complex $[Cd_{10}(SR)_{16}]^{4+}$ is formed. When the μ_3-thiolate at the pyramidal plane of this complex is replaced by S, the structure $[S_4Cd_{10}(SR)_{12}]^0$ is formed. The structure $[S_4Cd_{10}(SR)_{16}]^{4-}$ is produced if four SR ligands coordinate to each Cd atom at the four vertexes of the $Cd_{10}S_{16}$ tetrahedron. This decanuclear Cd cluster is well-known as $[S_4Cd_{10}(SCH_2CH_2OH)_{16}]^{4-}$ with mercaptoethanol ligand[10] and as $[S_4Cd_{10}(SPh)_{16}]^{4-}$ with thiophenol ligand.[11] When four and five Cd atoms are located on each side of a triangular pyramid, larger clusters in this series such as $[S_{13}Cd_{20}(SR)_{22}]^{8-}$ and $[S_{28}Cd_{35}(SR)_{28}]^{14-}$ are constructed, respectively.[12] The latter pyramidal cluster seems unstable, because the four Cd atoms

10.1021/jp013445y CCC: $22.00
Published on Web 03/07/2002

TABLE 1: Structural Classification of Polynuclear Cd Complexes and Their Excitation Energies

no. of atoms					excitation energy/eV			
					MOPAC		experimental	
Cd	Cd + S	diameter/Å	chemical formula	structure[a]	(HOMO−LUMO)	FDQW[b]	aliphatic thiolate	thiophenolate
1	5	6.2	$[Cd(SR)_4]^{2-}$	Mix	9.289	6.752	5.17	4.40
4	14	8.7	$[Cd_4(SR)_{10}]^{2-}$	ZB-t	7.556	5.503		4.98
4	15	8.9	$[SCd_4(SR)_{10}]^{4-}$	W	6.528	5.427		
4	17	9.3	$[SCd_4(SR)_{12}]^{6-}$	ZB-c	8.136	5.293	4.77	
8	25	10.6	$[SCd_8(SR)_{16}]^{2-}$	Mix	5.458	4.902	4.43	
10	30	11.2	$[S_4Cd_{10}(SR)_{16}]^{4-}$	ZB-t	6.398	4.730	4.88	4.25
13	41	12.5	$[S_4Cd_{13}(SR)_{24}]^{6-}$	ZB-c	5.623	4.454		
14	41	12.5	$[S_5Cd_{14}(SR)_{22}]^{4-}$	W	3.691	4.454		
17	49	13.2	$[S_4Cd_{17}(SR)_{28}]^{2-}$	Mix	4.365	4.308	4.28	
20	55	13.7	$[S_{13}Cd_{20}(SR)_{22}]^{8-}$	ZB-t	5.225	4.217		3.53
28	83	15.8	$[S_{13}Cd_{28}(SR)_{42}]^{12-}$	ZB-c	4.011	3.921	(3.82)	
32	86	15.9	$[S_{14}Cd_{32}(SR)_{36}]^{0}$	Mix	4.490	3.897	3.82	3.46
35	91	16.2	$[S_{28}Cd_{35}(SR)_{28}]^{14-}$	ZB-t	3.126	3.860		(3.35)
54	134	18.5	$[S_{32}Cd_{54}(SR)_{48}]^{4-}$	Mix		3.626	3.70	
55	147	19.1	$[S_{28}Cd_{55}(SR)_{64}]^{10-}$	ZB-c		3.574		
92	239	22.4	$[S_{55}Cd_{92}(SR)_{92}]^{18-}$	ZB-c		3.335	(3.35)	

[a] Mix, ZB−W mixed arrangement; ZB-t, tetrahedron by ZB arrangement; ZB-c, cuboctahedron by ZB arrangement; W, wurtzite arrangement. [b] FDQW: excitation energy calculated with the finite depth quantum well model[20] in effective mass approximation.

at the vertex tend to leave the cluster through the MO calculation process with geometry optimization.

(2) ZB Cuboctahedron. Cuboctahedron is one of the polyhedrons that has a shape like a sphere.[13] Tetrahedral $Cd(SR)_4$ is the smallest complex and corresponds to two shells in this series. When the center atom is Cd, the structures in this series will be $[S_4Cd_{13}(SR)_{24}]^{6-}$ and $[S_{28}Cd_{55}(SR)_{64}]^{10-}$, corresponding to four and six shells, respectively. When the center atom is S, a minimum cluster would be $[S_1Cd_4(SR)_{12}]^{6-}$ of three shells, and $[S_{13}Cd_{28}(SR)_{42}]^{12-}$ and $[S_{55}Cd_{92}(SR)_{92}]^{18-}$ would be formed, corresponding to five and seven shells, respectively.[13]

(3) Wurtzite Cluster. The smallest cluster of wurtzite arrangement may be $[S_1Cd_4(SR)_{10}]^{4-}$, which has the same framework as DABCO (1,4-diazabicyclo[2.2.2]octane). The wurtzite arrangement in a bulk crystal is thermodynamically stable because the material density of W is higher than that of ZB. However, the W-type cluster of CdS has not been reported so far.[8] Molecular orbital calculation revealed that this instability stems from the large electric polarization that must be contained in a small cluster. The calculated dipole moment for W-type $[S_1Cd_4(SH)_{10}]^{4-}$ is 14.0 D, while that of ZB-type $[Cd_4(SH)_{10}]^{2-}$ is 1.5 D. To form W-type Cd-thiolate clusters, this large dipole moment of CdS framework should be neutralized by certain methods, as will be described below.

(4) ZB−W Mixed Structure. Most polynuclear Cd complexes reported in the literature have the framework of the ZB−W mixed structure. This is explained by the results stated above. Namely, the large dipole moment of W structure is neutralized by gathering four W-type units to form a cluster of T_d symmetry. Thus, four of the smallest W cluster $[S_1Cd_4(SR)_{10}]^{4-}$ are condensed to form $[S_1Cd_8(SR)_{16}]^{2-}$, where the S atom at the center is common for four W cluster units and the next four Cd atoms of the center are common for each three W cluster units. This eight nuclear cluster has been reported to be stable in aqueous solution.[14] When center atom is Cd, a 17 nuclear cluster, $[S_4Cd_{17}(SR)_{28}]^{2-}$, is formed. The crystal structures of the $Cd_{17}S_{32}$ clusters with mercaptoethanol ligands,[15] $[S_4Cd_{17}(SCH_2CH_2OH)_{26}]^0$, and with thiophenol ligands,[16] $[S_4Cd_{17}(SPh)_{28}]^{2-}$, have been already analyzed. When a ZB framework of Cd_4 (i.e., adamantane framework) is located at the center to condense four W-type units, a 32 nuclear cluster, $[S_{14}Cd_{32}(SR)_{36}]^0$, is formed. The dipole moment calculated for this cluster was almost null, namely 0.6 D. Actually existence of Cd_{32} clusters with mercaptopropanol,[17] $[S_{14}Cd_{32}(SCH_2CH(OH)CH_3)_{36}]$, and thiophenol,[18] $[S_{14}Cd_{32}(SPh)_{36}]$, have been reported.

The polynuclear Cd thiolate complexes mentioned above are listed in Table 1 in the order of size. In this table, diameter, d, is calculated from the number of frame atoms, N_{sc}. That is, $d = 5.82(3N_{sc}/4\pi)^{1/3}$ based on the averaged atomic volume of ZB crystal.[13,19] Excitation energy can be calculated by using the finite depth quantum well model,[20] where an empirical relationship between the energy shift and the particle size[19] was used for convenience. Experimental values are evaluated from the reported absorption peak.[21]

For these clusters, semiempirical molecular orbital calculation with the parametric method 3 (PM3)[22] in MOPAC93, -97, and -2000 packages[23] has been used. In Table 1, the energy differences between LUMO and HOMO calculated for SH ligand are listed. In the MO calculation, geometry optimization was usually used, but some geometrical parameters were fixed for large clusters and for unstable molecular structures. The excitation energy estimated from the MO calculation decreased continuously with increasing size in each classified series. The excitation energies of the HOMO−LUMO difference tend to become higher than those of the experimental observation.

Effect of Ligands on the Electronic States. Since benzene is a kind of chromophore, thiophenol ligand may interact electronically with CdS nanoparticles. Actually, the absorption peak in the UV−vis spectra of $[S_{14}Cd_{32}(SR)_{36}]^0$ cluster with thiophenol ligand locates at 358 nm,[16] while that with mercaptopropanol ligand locates at 325 nm.[15] The experimental data listed in Table 1 clearly show that the size dependency of the excitation energy for clusters with thiophenol ligands differs from that for those of aliphatic ligands, as stated in our previous report.[19] To investigate the nature of the decrease in the excitation energy, MO calculation was performed for polynuclear Cd complexes with thiophenol ligand.

For three kinds of ligand, −SH, $-SCH_2CH_2OH$, and −SPh, the energy levels of $[S_1Cd_8(SR)_{16}]^{2-}$ cluster were calculated by the PM3 method. Figure 1 shows the density of states, which is fractionated to each kind of atom, that is, S, Cd, and other elements. Summing the square of the MO coefficient over all atoms for each energy level in 0.2 eV width and then doubling it to account for the number of electrons calculate the density of states. The contributions of the Cd 5s in LUMO and S 3p in HOMO became dominant with the increase of the cluster size.

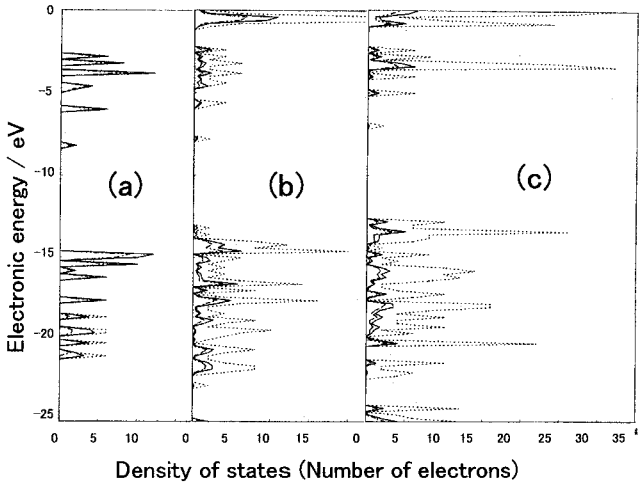

Figure 1. Density of states for $[S_1Cd_8(SR)_{16}]^{2-}$ clusters with the ligand SR of (a) $-$SH, (b) $-SCH_2CH_2OH$, and (c) $-$SPh. The dashed line shows the number of electrons on the S atom, the solid line represents that on both S and Cd atoms, and the dotted line stands for the total number involving other atoms, H, C, and O.

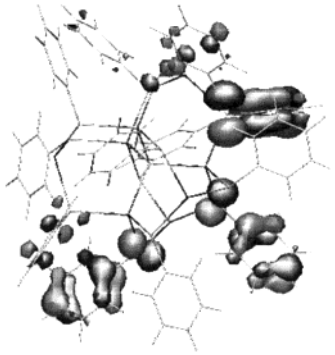

Figure 2. Molecular orbital for HOMO of the Cd_8S_{17} cluster capped with a phenyl group $[S_1Cd_8(SPh)_{16}]^{2-}$.

This observation is consistent with the reported result based on CNDO/2 calculation.[3]

By comparing parts a and b of Figure 1, the HOMO state at about -15 eV shifts toward a higher energy, resulting from the coordination of alkanethiolate. Three kinds of density of states in Figure 1b showed similar curves, indicating that the electrons distribute both to CdS and ligand carbon atoms at this energy band. Thus, MO calculation illustrates that the interaction of the CH_2 group of mercaptoethanol with the CdS framework is different from that with H atom. Figure 1c shows that the electronic interaction increases further when a phenyl group binds to the CdS framework. Figure 2 shows the details of the interaction by using molecular orbital representation for HOMO of the $[S_1Cd_8(SPh)_{16}]^{2-}$ cluster. Electrons in the p-orbital of S atoms in CdS frame interact with the π-orbital of benzene moiety to form an anti-π-bond. This electronic interaction must be the origin of the upper shift of the HOMO of the CdS frame in Figure 1c. This observation is consistent with the result obtained by ab initio calculation for $[S_4Zn_{10}(SPh)_{12}]^0$.[24]

Since the Cd_8S_{17} cluster seems too small to recognize the effect of a surface-capped phenyl group, the $Cd_{31}S_{40}$ cluster was calculated as the largest cluster within the limitation of the facility used in the present study. The structure of this cluster $[S_{28}Cd_{31}(SR)_{12}]^{6-}$ shown in Figure 3 was formed by removing the four vertex Cd atoms from the $[S_{28}Cd_{35}(SR)_{28}]^{14-}$ cluster of a triangular pyramid. For a cluster of this size, the unique properties observed in the quantum well model of nanoparticles could be represented by the result of the MO calculation. That is, the LUMO has large MO coefficients at inner Cd atoms, while the HOMO has large coefficients at surface S atoms. This observation in the electron distribution corresponds to that in the quantum well model. For the calculation by the spherical quantum well model, conduction band electrons in the 1S state locate mainly at the center of the particle, and valence band holes in the 1S state also locate at the center.[20] It should be noted that the latter means that electrons in the 1S valence state locate near the surface of the particle.

Figure 4 shows the comparison between $-$SH and $-$SPh ligands for the density of state around the band gap energy of $Cd_{31}S_{40}$ clusters. The HOMO level at about 3 eV shifts to a higher energy by changing the termination from hydrogen to phenyl. The densities of both Cd and S atoms at the valence band edge increased on the phenyl termination. The same pattern observed for three lines in this region indicates that electrons distribute to the phenyl groups by a certain fraction at every energy level corresponding to the valence band. Total electron densities at Cd and S atoms in this region decreased significantly. This corresponds to the increase of the size that confines holes in the spherical quantum well and then the decreased shift of the valence band edge to a lower energy by the size quantization. On the other hand, the densities at Cd and S atoms in the virtual MOs above 7 eV, which correspond to the density of states of the conduction band, were increased upon coordination of the phenyl group.

The above discussion explains the experimentally observed decrease in the excitation energy with capping by phenyl groups. That is, the electronic interaction of phenyl with the surface S atom through anti-π-bond raises the maximum energy of the valence band, and thus, the excitation energy is decreased. This concept of the energy shift is illustrated in Figure 5, where experimental values of band gap energy for 1.6 nm CdS clusters are shown as the effect of the phenyl group at the surface. The surface phenyl group raises the valence band edge by 10% in this particular case.

Nanocrystalline Dimer and Intercluster Interaction. Since the peak wavelength in the absorption spectrum of CdS nanoparticles shifts by aggregation in a film,[25] it is suggested that the excitation energy decreases when CdS nanoparticles get close to each other. However, as far as we know, precise experimental evidence for the particle interaction has not been reported yet, because of the difficulty in the experiment. Then, it is interesting to analyze the interparticle interaction by molecular orbital calculation. The usual closed shell SCF calculation for cluster dimers showed that the electron density for each energy state is similar to that of the corresponding monomer. Since the CI (configuration interaction) analysis in the semiempirical method merely causes a complexity for the analysis, we adopted the open shell SCF calculation to investigate the intramolecular interaction, where HOMO and LUMO orbitals are occupied with one electron in the singlet spin-state configuration. Although this method corresponds to the calculation of the single-electron excited state, the obtained electron density and energy levels likely reflect the electronic interaction between two particles in the cluster dimer. We modeled nanoparticle dimers by linking two $Cd_{17}S_{32}$ clusters by $-$S$-$, $-$SS$-$, and $-SCH_2S-$ bonds. Figure 7 shows the density of states for the dimers and the corresponding monomer for comparison. In the case of the S-linking, the HOMO electron delocalized over the surface S atoms was gathered on the linking S atom, which is the common S atom for each monomer unit. Thus, the HOMO level rises, as shown in Figure 7b. When the

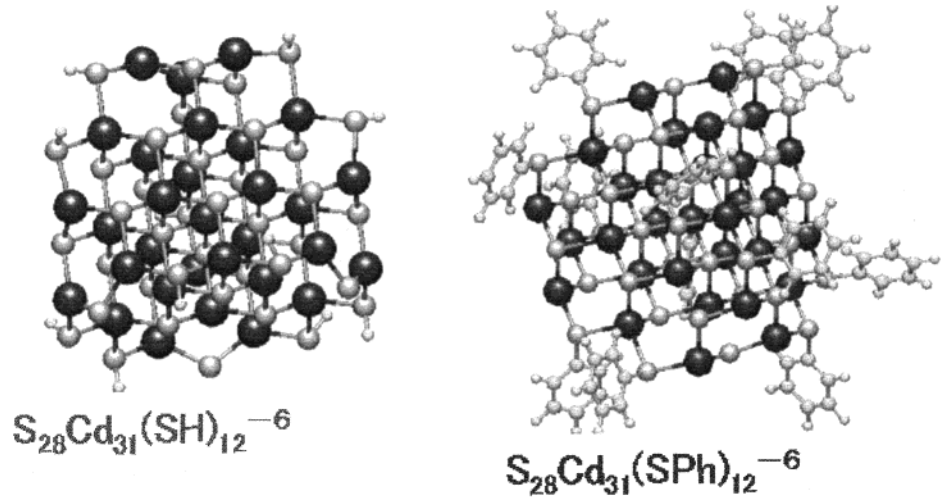

Figure 3. Chemical structures of the $Cd_{31}S_{40}$ clusters with −SH and −SPh ligands.

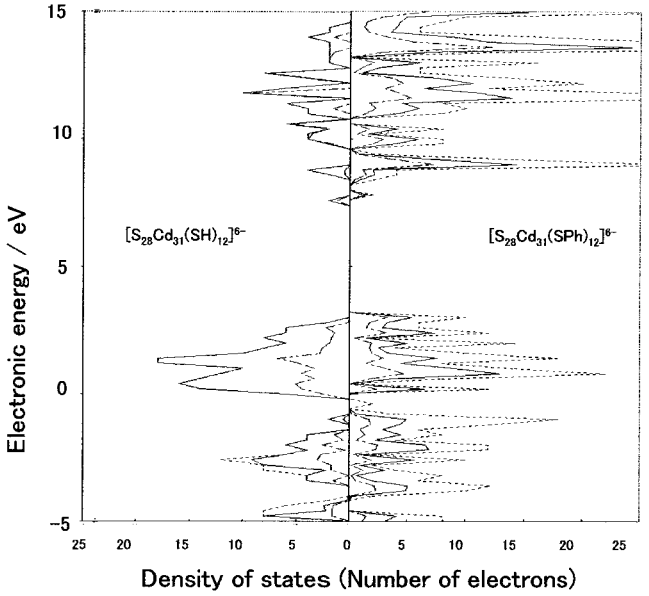

Figure 4. Effect of the phenyl ligand on the fractionated density of states of $[S_{28}Cd_{31}(SR)_{12}]^{6-}$ clusters. The dashed line shows the number of electrons on the Cd atom, the solid line represents that on both Cd and S atoms, and the dotted line stands for the total number involving other atoms, H and C.

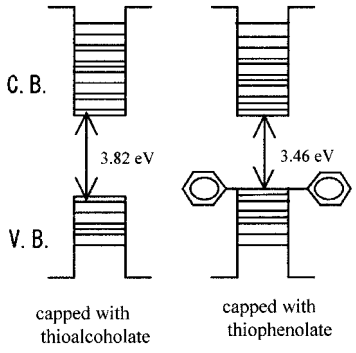

Figure 5. Schematic energy level diagram of 1.6-nm CdS nanoparticles showing the effect of phenyl-capping on the electronic states.

−SS− bond links two clusters, the high electron negativity of the −SS− group raises the HOMO level further, as shown in Figure 7c. Figure 7d indicates that this effect declined when the CH_2 group is present between the two −SS− atoms. The energies of HOMO−LUMO difference for these four molecules

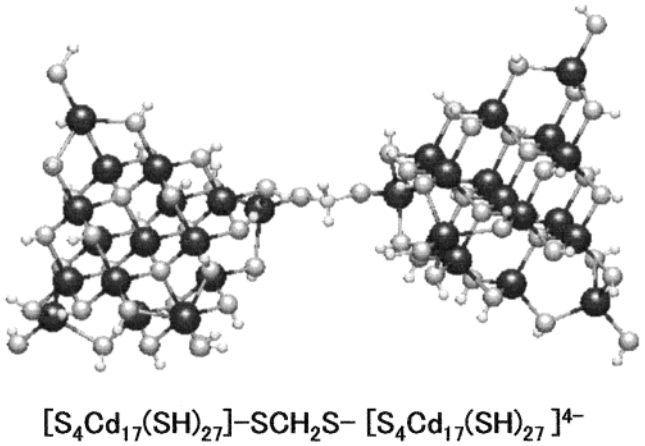

Figure 6. Model for a CdS cluster dimer bonded with a methylene group.

were 2.89, 3.40, 2.53, and 3.20 eV, showing no clear decrease with the dimer formation. However, the shape of the density of states around −5 eV is slightly modified if part a is compared with parts b, c, and d in Figure 7. As for the change in the excitation energy, a clear explanation may not be presented because of the limitation in the HF SCF calculation. However, solid-state physics tells us that the transition dipole for electronic excitation is restricted in the unit cell of crystalline lattice. This is evidenced by the observation that the oscillator strength is independent of the size.[25] Then, it is expected that the electronic interaction between nanocrystallites is significantly small.

Conclusions

A semiempirical MO calculation (MOPAC-PM3) was applied to investigate the effects of crystal arrangement, phenyl capping, and dimer formation for CdS nanoparticles as follows.

We classified the structure of nanoparticles into four groups and showed that the size effect on HOMO−LUMO energy difference is observed in each group. ZB−W mixed structure is found to be stable because of the special neutralization of the high dipole moment inherent in the W structure unit. The triangular pyramid of the Cd_{35} sulfide cluster is suggested to be unstable to hold the vertex Cd atoms.

An electronic interaction between the CdS framework and the surface-capped phenyl group may take place through the anti-π-bond interaction between the surface S atom and the

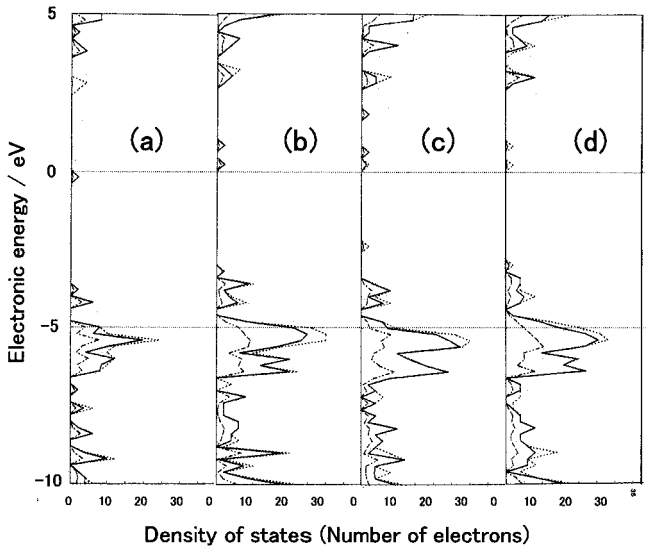

Figure 7. Effect of linking $Cd_{17}S_{32}$ clusters with (b) −S−, (c) −SS−, and (d) $-SCH_2S-$ on the electronic states. Part a shows monomer $[S_4Cd_{17}(SH)_{28}]^{2-}$, whose energy was moved upward by 1 eV for comparison. The chemical structure of part d is shown in Figure 6. The dashed line shows the number of electrons on the Cd atom, the solid line represents that on both Cd and S atoms, and the dotted line stands for the total number involving H and C atoms.

benzene moiety to extend the electron distribution over the surface phenyl groups.

The effect of dimer formation on the electronic energy of nanoparticles was not observed in the scope of the present calculation with the open shell SCF method.

Acknowledgment. The present work is partly defrayed by the Grant-in-Aid for Scientific Research on Priority-Area-Research of "Single Organic Nanoparticles" from the Japanese Ministry of Science, Education and Culture.

References and Notes

(1) (a) *Semiconductor Nanoclusters—Physical, Chemical, and Catalytic Aspects*; Kamat, P. V., Meisel, D., Eds.; Elsevier: Amsterdam, 1997. (b) *Physics, Chemistry and Application of Nanostructures*; Borisenko, V. E., Filonov, A. B., Gaponenko, S. V., Gurin, V. S., Eds.; World Scientific: Singapore, 1997.

(2) Gurin, V. S. *J. Phys. Conden. Mat.* **1994**, *6*, 8691; *J. Phys. Chem.* **1996**, *100*, 869.

(3) Okano, K.; Hayashi T.; Miyamoto, A. *Jpn. J. Appl. Phys.* **1999**, *38*, 6107.

(4) Kuz'mitskii, M. V. A.; Gael', V. I.; Filatov, I. V. *J. Appl. Spectrosc.* **1996**, *63*, 594.

(5) Gurin, V. S. *Solid. State. Commun.* **1999**, *112*, 631.

(6) Eichkorn, K.; Ahlrichs, R. *Chem. Phys. Lett.* **1998**, *288*, 235.

(7) Nosaka, Y. *Curr. Top. Colloid. Interface Sci*. **1997**, *1*, 225; Nosaka, Y.; Ohta, N.; Fukuyama, T.; Fujii, N. *J. Colloid, Interface Sci.* **1993**, *155*, 23.

(8) Eychmueller, A. *J. Phys. Chem. B* **2000**, *104*, 6514.

(9) Dean, P. A. W.; Vittal, J. J. *Inorg. Chem*. **1986**, *25*, 514.

(10) Strickler, P. *Chem. Commun*. **1969**, 655.

(11) Dance, I. G.; Choy, A.; Scudder, M. L. *J. Am. Chem. Soc.* **1984**, *106*, 6285.

(12) Wang, Y.; Herron, N. *J. Phys. Chem*. **1991**, *95*, 525.

(13) Lippens, P. E.; Lannoo, M. *Phys. Rev.* **B 1989**, *39*, 10935.

(14) Nosaka, Y.; Shigeno, H.; Ikeuchi, T. *Surf. Rev. Lett.* **1996**, *3*, 1209.

(15) Vossmeyer, T.; Reck, G.; Katsikas, L.; Haupt, E. T. K.; Schulz, B.; Weller, H. *Science* **1995**, *267*, 1476.

(16) Burgi, H.-B.; Gehrer, H.; Strickler, P.; Winkler, F. K. *Helv. Chim. Acta* **1976**, *59*, 2558.

(17) Vossmeyer, T.; Reck, G.; Schulz, B.; Katsikas, L.; Weller, H. *J. Am. Chem. Soc*. **1995**, *117*, 12881.

(18) Herron, N.; Calabrese, J. C.; Farneth, W. E.; Wang, Y. *Science* **1993**, *259*, 1426.

(19) Nosaka, Y.; Shigeno, H.; Ikeuchi, T. *J. Phys. Chem*. **1995**, *99*, 8317.

(20) Nosaka, Y. *J. Phys. Chem*. **1991**, *95*, 5054.

(21) Tuerk, T.; Resch, U.; Fox, M. A.; Vogler, A. *J. Phys. Chem*. **1992**, *96*, 3818; the individual literature cited above.

(22) Stewart, J. J. P. *J. Comput. Chem*. **1989**, *10*, 209; **1991**, *12*, 320.

(23) MOPAC93 and MOPAC97 in WinMOPAC; MOPAC2000 (Version 1.32) in WinMOPAC 3.0 Professional, Fujitsu Ltd. Tokyo.

(24) Bertoncello, R.; Bettinelli, M.; Casarin, M.; Maccato, C.; Pandolfo, L.; Vittadini, A. *Inorg. Chem*. **1997**, *36*, 4707.

(25) Vossmeyer, T.; Katsikas, L.; Giersig, M.; Popovic, I. G.; Diesner, K.; Chemseddine, A.; Eychmueller, A.; Weller, H. *J. Phys. Chem.* **1994**, *98*, 7665.